Conformal growth of Mo/Si multilayers on grating substrates using collimated ion beam sputtering

D.L. Voronov,[1],* P. Gawlitza,[2] R. Cambie,[1] S. Dhuey,[1] E.M. Gullikson,[1] T. Warwick,[1] S. Braun,[2] V.V. Yashchuk,[1] and H.A. Padmore[1]

[1]Lawrence Berkeley National Laboratory, 1 Cyclotron Road, Berkeley, CA 94720, USA

[2]Fraunhofer Institute for Material and Beam Technology, Winterbergstraße 28, 01277 Dresden, Germany

*email: dlvoronov@lbl.gov

Abstract

Deposition of multilayers on saw-tooth substrates is a key step in the fabrication of multilayer blazed gratings (MBG) for extreme ultraviolet and soft x-rays. Growth of the multilayers can be perturbed by shadowing effects caused by the highly corrugated surface of the substrates, which results in distortion of the multilayer stack structure and degradation of performance of MBGs. To minimize the shadowing effects we used an ion-beam sputtering machine with a highly collimated atomic flux to deposit Mo/Si multilayers on saw-tooth substrates. The sputtering conditions were optimized by finding a balance between smoothening and roughening processes in order to minimize degradation of the groove profile in the course of deposition and at the same time to keep the interfaces of a multilayer stack smooth enough for high efficiency. An optimal value of energy of 200 eV for sputtering Kr^+ ions was found by deposition of test multilayers on flat substrates at a

range of ion energies. Two saw-tooth substrates were deposited at energies of 200 eV and 700 eV for the sputtering ions. It was found that reduction of the ion energy improved the blazing performance of the MBG and resulted in a 40% gain in the diffraction efficiency due to better replication of the groove profile by the multilayer. As a result of the optimization performed, an absolute diffraction efficiency of 28.8% was achieved for the 2nd blaze order of the MBG with a groove density of 7350 lines/mm at a wavelength of 13.5 nm. Details of the growth behavior of the multilayers on flat and saw-tooth substrates are discussed in terms of the Linear Continuous Model of film growth.

Introduction

Highly efficient diffraction gratings capable of operating at near-normal incidence are of great importance for a variety of soft x-ray and extreme ultraviolet (EUV) applications such as astronomy, microscopy, EUV lithography, and high-resolution spectroscopy [1]. A most promising solution is a multilayer blazed grating (MBG) which can deliver most of the diffracted light in a high diffraction order. Fabrication of a MBG includes manufacture of a saw-tooth substrate followed by deposition of a multilayer reflector on it. Both the steps are significant technological challenges because the short wavelength of soft x-ray or EUV radiation imposes strict requirements on grating quality. To realize the full potential of MBGs, a saw-tooth substrate should have an atomically smooth surface of the blaze facets and a perfect triangular groove profile, as well as good reproduction of the groove shape by all the interfaces of the overlaying multilayer.

Recent progress in fabrication of saw-tooth substrates by anisotropic wet etch of silicon single crystals provided very high quality saw-tooth substrates, and diffraction efficiency higher than 37% was achieved for a 5000 line/mm MBG in the 1st order at a wavelength of 13.5 nm [2], relevant for EUV lithography applications. However the achieved efficiency is still almost a factor of two lower than the theoretical one. Simulations of diffraction efficiency showed that distortion of the groove profile during multilayer deposition is one of main causes of efficiency degradation [3]. While growth of MLs on flat substrates is a well established process, deposition of MLs on the highly corrugated surface of a saw-tooth substrate still remains a challenge to be adequately addressed.

Two main negative processes of shadowing and smoothing affect the groove profile during ML growth. The shadowing of an atomic flux by surface relief features can result in column-like growth of a coating with very perturbed interfaces of a ML. This negative tendency can be relatively easily overcome for a flat substrate when surface imperfections caused by surface roughness or local fluctuations of the atomic flux are relatively small and can be smoothed out, provided a surface relaxation process is in effect. Moreover a choice of normal deposition geometry, when trajectories of deposited atoms are perpendicular to a substrate surface, mitigates shadowing effects.

The shadowing problem becomes much more severe for the highly corrugated surface of a saw-tooth substrate, which can provoke the shadowing even for the optimized deposition geometry. In contrast to flat substrates it is not possible to provide a normal

deposition for all parts of the structured surface and avoid the local oblique deposition that leads to the enhancement of shadowing. This problem can be crucial for the soft x-ray MBG, where extremely high groove density is required in order to obtain very high spectral resolution [4]. In this case the grating period should be between 100-200 nm and such a substrate should be coated with a ML with a total thickness of 200-400 nm. One needs therefore to provide suppression of the shadowing effects otherwise the structure of the ML stack will be perturbed greatly and the blazed grating performance will be destroyed.

We used dc-magnetron sputtering for MBG fabrication earlier [2,3]. This technique works very well for deposition of MLs on flat substrates since it provides high stability of deposition rates and high uniformity of layer thickness over a substrate area which is very important for the ML performance. However, the large dimensions of a magnetron source and the short distance between a target and a substrate result in large divergence of the atomic flux coming to a substrate. Even if an average direction of atomic flux is perpendicular to the substrate surface the deposited atoms hit the surface at oblique angles. As a result of this it was not possible to avoid shadowing for the saw-tooth substrate and in practice, significant distortion of the ML stack is observed [3]. A collimated deposition is required to mitigate the shadowing problem. In this work we use an ion-beam sputtering machine which provides a highly collimated atomic flux at the substrate.

The other possible issue is the smoothing of multilayers, which although crucial for smoothing out atomic scale defects also can result in degradation of a triangular groove profile. The smoothening can be stimulated by a bombardment of the growing surface with energetic particles. Hence, a deposition process should be optimized in terms of energy of

deposited particles. In this paper we investigate capabilities of ion-beam sputtering techniques to control the growth of Mo/Si multilayers on ultra-dense saw-tooth substrates, and report on the first results of deposition optimization based on the analysis of multilayer growth at different energy of sputtering ions. We fabricated MBGs with groove density of 7350 lines/mm and investigated dependence of their performance on sputtering conditions.

2. Experiment

An ion-beam sputtering machine at the Fraunhofer Institute for Material and Beam Technology was used for deposition of Mo/Si multilayers on flat and saw-tooth substrates [5]. A schematic of the setup is shown in Fig. 1. Sputtering ions generated by an ion gun (1) hit the surface of a target (2) at the average angle of incidence, α. Sputtered atoms go through an aperture (3) and deposit onto a surface of the substrate (4) which moves across the aperture. The velocity of the substrate motion defines a time of substrate exposure against the atomic flux, and was chosen to provide deposition of one layer of Si or Mo in one substrate pass. The large distance of 500 mm between the target and the aperture provided a highly collimated atomic flux at the substrate. The largest possible variation of deposition angles at the substrate was estimated to be as low as 13º for the 80 mm wide sputter area on the target.

An incidence angle and the position of the aperture with respect to the target were optimized to provide the largest yield of sputtered atoms, and at the same time a lowest

possible energy of sputtered particles hitting the surface of the substrate. SRIM software [6] was used for simulation of sputtering of Si and Mo targets with Ar^+ and Kr^+ ions in order to obtain a distribution of the number and energy of sputtered particles over a take-off angle β, and dependence of the distribution on incidence angle, energy of the sputtering ions and other system parameters.

Most of the simulations were performed for the incidence angle α=60º which was found to be the most suitable for the machine used. Variation of the angle does not give a significant improvement in terms of the simulation criteria mentioned above.

The deposition of Mo/Si multilayers on flat and saw-tooth substrates was performed at different ion energies from 100-700 eV. The multilayers consisted of 50 or 30 bi-layers with a d-spacing (i.e. a bi-layer thickness) of approximately 7 nm and a Γ-ratio (i.e. a ratio of Mo layer thickness to the d-spacing) of about 0.45. Semiconductor quality silicon wafers were used as flat substrates, and silicon blazed gratings with a period of 136 nm and a blaze angle of 6º were used as saw-tooth substrates for the multilayer deposition. The gratings were fabricated with a nanofabrication process based on wet anisotropic etch of silicon single crystals [7,8]. The process included e-beam lithography patterning of resist on the surface of asymmetrically cut silicon wafers coated with a low-stress silicon nitride layer, transfer of the patterns to the nitride layer with reactive ion etching, followed by wet anisotropic etching of silicon, and finished with an isotropic chemical etch. The process results in a near atomically perfect facetted surface. The details of the silicon blazed grating fabrication process were described earlier [2].

The surface of the gratings and flat multilayers was characterized before and after the deposition with a Veeco Dimension-3100 Atomic Force Microscope (AFM). Surface morphology of the coatings was analyzed using a Linear Continuum Model (LCM) [9] which has been shown to work well for flat multilayer coatings [10,11]. According to the model, the kinetics of surface growth is described with the equation:

$$\frac{\partial \boldsymbol{h}(\boldsymbol{r},\boldsymbol{t})}{\partial \boldsymbol{t}} = -\sum_{\boldsymbol{n}} \nu_{\boldsymbol{n}} \nabla^{\boldsymbol{n}} \boldsymbol{h}(\boldsymbol{r},\boldsymbol{t}) + \eta(\boldsymbol{r},\boldsymbol{t}) \tag{1}$$

where $\boldsymbol{h}(\boldsymbol{r},\boldsymbol{t})$ is a surface height, $\boldsymbol{r}$ is a radius vector, $\boldsymbol{t}$ is a time of the deposition (or a coating thickness provided the deposition rate is constant), $\eta(\boldsymbol{r},\boldsymbol{t})$ is a white noise caused by fluctuations of the incoming atomic flux, $\nu_{\boldsymbol{n}}$ is a relaxation parameter, $\boldsymbol{n}$ is a relaxation exponent which depends on a relaxation mechanism which can be a viscous flow ($\boldsymbol{n}=1$), evaporation and condensation or downhill currents ($\boldsymbol{n}=2$), volume diffusion ($\boldsymbol{n}=3$), and surface diffusion ($\boldsymbol{n}=4$) [12,13].

According to the model a Power Spectral Density (PSD) spectrum of a coating grown on an ideal substrate is:

$$\boldsymbol{PSD}(\boldsymbol{f},\boldsymbol{d}) = \Omega \frac{1-\mathbf{exp}(-2\boldsymbol{d}\sum \nu_{\boldsymbol{n}} \boldsymbol{f}^{\boldsymbol{n}})}{\sum \nu_{\boldsymbol{n}} \boldsymbol{f}^{\boldsymbol{n}}} \tag{2}$$

where $\boldsymbol{f}$ is a spatial frequency, $\boldsymbol{d}$ is a film thickness, Ω is the strength of the white noise and corresponds to an atomic volume for amorphous materials, and $\nu_{\boldsymbol{n}}$ is a relaxation parameter which is related to a relaxation length, $\boldsymbol{l}$, via

$$\boldsymbol{l}^{\boldsymbol{n}-1} = \nu_{\boldsymbol{n}} \tag{3}$$

PSD evolution of a coating growing on an initially rough substrate ($\boldsymbol{PSD_{sub}} \neq 0$) is

$$\boldsymbol{PSD_{tot} = PSD_{film} + a^2 PSD_{sub}} \tag{4}$$

where $\boldsymbol{a}$ is a frequency dependent replication factor

$$\boldsymbol{a = \exp-(d\nu_n f^n)} \tag{5}$$

Flat multilayers were characterized by a small angle x-ray diffraction (SAXRD) technique in order to establish the parameters of the multilayers such as a d-spacing and Γ-ratio, and estimate the quality of the multilayers. The SAXRD data were used to calibrate deposition rates and deposition times for each value of energy of sputtering ions in order to provide a ML d-spacing of approximately 7 nm as required for an x-ray resonance wavelength of the multilayers around 13.5 nm.

Reflectance of the flat multilayers and diffraction efficiency of the MBGs in the EUV wavelength range were measured at Advanced Light Source (Beamline 6.3.2).

3. Results and discussion

3.1. Simulations of sputtering

Preliminary optimization of deposition of Mo/Si multilayers was performed using simulation of the sputtering of Mo and Si with Ar^+ and Kr^+ ions for energy of the sputtering ions within the range of 100-1000 eV. The aim of the optimization was to find the best sputter-deposition geometry and conditions which would provide, on the one hand, the

highest deposition rates and on the other hand, minimize bombardment of the coating surface with energetic particles, which can deliver a substantial amount of energy to the growing surface and stimulate relaxation processes.

From the simulation we found that angular distributions of sputtered Mo and Si atoms n(β) have a maximum at the takeoff angle $\beta \approx 90°$. In order to provide a maximum deposition rate, an aperture (3) was placed in the position which provided collection of the atoms sputtered at the takeoff angle close to the target normal (Fig. 1). The distributions are also affected by an incidence angle, but this is a minor effect, so an incidence angle of 60º was chosen for all further simulations and deposition experiments. Energy of the sputtering ions does not affect much the angle distributions, but does affect the sputter yield significantly. One should expect a reduction of the deposition rates for an ion energy of 200 eV by a factor of 3 - 4 as compared to an energy of 700 eV.

Energy distributions (dn/dE) of Mo and Si atoms sputtered with Ar^+ or Kr^+ ions with an energy of 200 eV and 700 eV are shown in Fig. 2. Only the particles sputtered within the takeoff angle range of $\beta = 90° \pm 20°$ were taken into account. This is similar to the experimental conditions, where only near normal takeoff particles could pass the aperture and reach the substrate, and hence can be considered as deposited particles. All raw distributions were obtained for the same number of incident ions. In order to take into account a variation of deposition rate with ion energy, the distributions were normalized to the deposition rate by dividing the raw data by the total number of deposited particles. In this way Fig. 2 illustrates the distributions of energy brought to a substrate surface while the

same thickness of a material is deposited under different sputtering conditions. It is seen that the switch from Ar^+ to Kr^+ ions does not affect the distributions noticeably, while reduction of ion energy results in some growth of the low-energy maximum and suppression of the high-energy tail of the distributions. The net effect on energy reduction is to decrease the average energy of the sputtered particles roughly by a factor of 1.5 for the low-energy sputter regime (see Table 1).

Energy distributions (dn/dE) of ions and neutrals of the sputtering gas backscattered from Mo and Si targets for an energy of the incident Ar^+ and Kr^+ ions of 200 eV and 700 eV are shown in Fig. 3. The distributions are normalized by the deposition rate by dividing the raw data by the number of deposited particles. It is seen that a backscattered particle distribution strongly depends on the sort and energy of the sputtering ions. A high-energy tail of the distribution of Ar atoms extends up to 400 eV, but is significantly suppressed for heavier Kr particles, and additional suppression is observed for low-energy Kr^+ sputtering (Fig. 3). As a result of that the average energy of the backscattered neutrals reduces significantly (Table 2).

However, the number of backscattered particles turns out to be much larger for the low-energy sputtering regime after the deposition rate normalization has been performed. The last probably does not make a difference for sputtering of Si since the total percentage of backscattered Kr from a silicon target does not exceed 0.1% of the total impinging on the surface, but can be substantial for the Mo sputtering when more than 5 % and 26 % of incident ions with energy 700 eV and 200 eV respectively scatter from the target. The

simulation shows that as compared to 700 eV Ar^+ bombardment, 200 eV Kr^+ bombardment results in the growing surface seeing a larger number of backscattered particles, but ions are delivered with a lower average energy. It is difficult to predict a net effect of this on multilayer growth, and direct experiments are necessary to investigate the impact of sputtering ion energy on the smoothing ability of multilayers.

To summarize the simulation part of this work, we found that an incidence angle of 60º and the take-off angle of 90º provide the best deposition geometry, and use of low-energy Kr^+ ions can be more suitable in terms of reduction of bombardment of growing surface with energetic particles. In the following sections we show a direct observation of the growth of the Mo/Si multilayer for Kr^+ ion energies of 200 eV and 700 eV.

3.2. Growth of Mo/Si multilayers on flat substrates

3.2.1. Optimization of Kr^+ ion energy

As was discussed above, reduction of the energy of the ions in a sputtering gas is expected to affect the smoothing ability of the multilayers and improve replication of a saw-tooth profile during the deposition. However at some point the relaxation processes can be depressed too much, and one should expect degradation of multilayer reflectance due to interface roughness build-up. In order to investigate a dependence of multilayer performance on ion energy and find a reasonable lower limit of the energy, we deposited a set of Mo/Si-50 multilayers composed of 50 bi-layers at an energy of Kr^+ ions of 100 eV -

700 eV. Quality of the multilayers was examined with small angle x-ray diffraction (SAXRD) at a wavelength of Cu-K_{α}. The SAXRD shows that in the high energy regime (400-700 eV) the best quality of the multilayer stack is achieved resulting in sharp and well defined Bragg peaks (Fig. 4). Some minor splitting and widening of the high-order Bragg reflections can be seen for ion energies of 300 eV and 200 eV indicating a degradation of the ML stack periodicity. A lowering of intensity of high-order Bragg peaks observed for the 200 eV multilayer indicates some increase of interface roughness. Reduction of the ion energy down to 100 eV results in drastic degradation of ML structure clearly manifested by the corresponding SAXRD (Fig. 5).

Measurements of EUV reflectance of the MLs are consistent with the SAXRD diffraction. Reflectance-versus-wavelength curves of the multilayers are shown in Fig. 5a, and dependence of the peak reflectance of the mirrors on the Kr^+ ion energy is depicted in Fig. 5b. The multilayers deposited at the high energies (300-700 eV) demonstrate a reflectance higher than 65%. Some minor variation of the reflectance values of the MLs is probably caused by differences in the resonant wavelengths due to slight deviation of d-spacing and Γ-ratio of the ML stacks from nominal ones (Fig. 4a). It is seen that slight imperfections of the ML stack observed with SAXRD for the 300 eV sample (Fig. 4) do not affect EUV performance of the mirror, while poor quality of the 100 eV ML stack resulted in distortion of the shape of the reflectance-versus-wavelength curve (Fig. 5a) and reduction of the peak reflectance down to 50%. Since the 200 eV sample still has a high reflectance of 62.5%, this ion energy of 200 eV was considered as a practical lower limit for Kr^+ ion energy for deposition of the multilayer on a saw-tooth substrate.

3.2.2. Impact of Kr^+ ion energy on surface dynamics on flat multilayers

In order to investigate the impact of ion energy on the multilayer growth and the grating performance, two Mo/Si multilayers composed of 30 bi-layers were deposited on saw-tooth substrates at the Kr^+ ion energy of 200 eV and 700 eV. The results will be discussed in the next section. Identical Mo/Si-30 multilayers were deposited on flat silicon substrates and served as witnesses. The witness multilayers were characterized with AFM in order to investigate intrinsic surface deposition dynamics of the Mo/Si coatings grown on flat substrates. The AFM images of a top surface of the flat witnesses are shown in Fig. 6. As was expected the reduction of ion energy resulted in some build-up of the top surface roughness which correlates with increasing interface roughness of the multilayer stack. PSD spectra of the top surface of the multilayers (Fig. 7) provide information on surface roughness in the spatial frequency domain. The PSD spectrum of the multilayer grown in the low-energy sputtering regime (200 eV) is shifted towards higher frequencies; at the same time a high frequency part of the spectrum is increased as compared to the one for the high-energy (700 eV) regime. This indicates that ion energy affects not only the smoothening processes but also roughening ones.

Quantitative analysis of PSD spectra of the multilayers was performed with a Linear Continuum Model using formulas (1,2). For simulations of PSD spectra we assumed re-sputtering and surface diffusion as relevant relaxation processes characterized with the exponents n=2 and n=4 respectively, while viscous flow (n=1) and volume diffusion (n=3)

were not allowed. This assumption seems reasonable for room temperature deposition and was found to work well for the deposition of multilayers and other coatings with ion-beam sputtering [10,11,14]. Values of fitting parameters which characterize white noise roughening, Ω, re-sputtering (ν_2), and surface diffusion relaxation (ν_4) for both the ion energies are listed in the Table 3. We found that both the exponents n=2 and n=4 contribute to relaxation processes resulting in a slope of the PSD spectra at high frequencies. The contribution of the mechanisms can be estimated with the ratio $\nu_2(2\pi f)^2/\nu_4(2\pi f)^4$ which shows that surface diffusion dominates for frequencies higher than $\boldsymbol{f}$=0.01 nm^{-1}, while re-sputtering contributes to the smoothening at lower frequencies.

LCM assumes a deposition process as a stochastic rain of atoms arriving to a substrate surface. In this case the strength of the white noise has a physical meaning in terms of an atomic volume which is about 0.02 nm^3 for Si atoms. However the value of a white noise strength parameter, Ω, obtained with our simulations exceeds the atomic volume by many times (Table 3). This indicates that additional non-stochastic roughening mechanisms such as island growth are relevant for the multilayer growth. Tong and Williams assumed that such kind of roughening could be frequency dependent in a similar way to smoothening processes [9]. They suggested to model island growth roughening with exponents n=1 and/or n=3, and strength parameters ν_1 or/and ν_3 which have an opposite sign to the smoothening parameters ν_2 and ν_4. Table 4 shows the simulation parameters obtained with the model accounting for a roughening mechanism with n=1 (incorporation of the roughening exponent n=3 was found to affect the results negligibly weakly, so the corresponding strength parameter ν_3 was assumed to be ν_3=0).

Comparison of the fitting parameters for both the models (Table 3 and Table 4) reveals a significant discrepancy in values of the relaxation parameters, ν_2 and ν_4. This indicates that the models are still probably oversimplified, and the parameter values should not be considered as absolute ones. A more sophisticated model is necessary in order to obtain the growth parameter values with better precision. However both the models clearly show a tendency for reduction of the smoothening parameters, ν_2 and ν_4, and an increase of roughening parameters, Ω and ν_1, with ion energy reduction. Reduction of the sputter ion energy results in suppression of relaxation processes and at the same time enhancement of roughening processes. The last seems reasonable because heterogeneous island nucleation can be driven by bombardment of a surface with energetic particles. The bombardment can result in surface defect formation and can facilitate nucleation, resulting in an increase of the number of nuclei and reduction of island dimensions and ultimately the net roughness after island coalescence has occurred. On the contrary, suppression of the high energy tails of the energy distributions of sputtered and back-scattered particles in this study (Fig. 2 and Fig. 3) can be a reason for the roughness built-up.

While attenuation of the smoothening process is desired for multilayer grating efficiency, the resulting roughening is undesirable in terms of multilayer Bragg reflectance. Finding a reasonable balance between the smoothening and roughening processes is a matter of a process optimization. In our case the net rms roughness measured over a 2 μm×2μm area increased from 0.20 nm to 0.26 nm for 700 eV and 200 eV respectively (Fig. 6). Assuming the same roughness behavior for the multilayer interfaces the obtained

roughness build-up seems quite reasonable in terms of reduced reflectivity for a wavelength of 13.5 nm.

3.3. Growth of Mo/Si multilayers on saw-tooth substrates

Two MBG were fabricated by deposition of Mo/Si multilayers on saw-tooth substrates with a blaze angle of 6º and groove density of 7350 lines/mm. The Mo/Si-30 multilayers composed of 30 bi-layers and were deposited by ion-beam sputtering at a Kr^+ ion energy of 200 eV and 700 eV. Cross-section TEM images of the gratings shown in Fig. 8 reveal the internal structure of the multilayer stacks. Due to the highly collimated flux of sputtered atoms arriving at the saw-tooth substrate, the shadowing effects are minimal, which results in continuous layers of the coating with almost no breaks as compared to the multilayers deposited with magnetron sputtering where typically there is a highly divergent atomic flux [3]. The AFM and TEM confirmed high smoothness of the blazed facet surface and perfect triangular profile of the grooves of the saw-tooth substrates (Fig. 8). However, initially saw-tooth grooves suffer a gradual smoothing in the course of multilayer deposition, for both ion energies of 200 eV and 700 eV. Degradation of the groove profile increases with the sputter ion energy, and the top surface for the 700 eV grating was found to be significantly affected by the smoothening (Fig. 9).

The groove profile degradation caused by the multilayer deposition is clearly manifested on the PSD spectra as a decay of the high-frequency harmonics of the PSD function calculated for the grating surface. Fig. 10 shows that the decay is much more

pronounced for the 700 eV sample. We applied the LGM for quantitative characterization of the PSD decay using as variables the value of the smoothening exponent, $\boldsymbol{n}$, and of a frequency dependent replication factor, $\boldsymbol{a}(f)$, (see formula 5). The replication factor is essentially a spatial frequency filter, which suppresses the high frequency part of a PSD spectrum. Fitting experimental PSDs with the equation (4) allows us to find a value of the relaxation exponent, $\boldsymbol{n}$, which is the main parameter that describes the smoothening process. For the simulations we used experimental PSD spectra of the saw-tooth substrates (PSD_{sub}) and multilayer coated gratings (PSD_{tot}). PSD functions of flat multilayer witnesses (Fig. 7) were used as an intrinsic multilayer PSD_{film}. Since the standard deviation of a corrugated surface of the saw-tooth substrates is much higher than roughness of the flat multilayer, a contribution of intrinsic $\boldsymbol{PSD_{film}}$ in total $\boldsymbol{PSD_{tot}}$ is very small and in fact can be neglected. The replication factor is determined by a ratio: $\boldsymbol{a}^2 \approx \boldsymbol{PSD_{tot} / PSD_{sub}}$. This simplification allows use of one-dimensional PSD functions instead of the isotropic two dimensional ones in formulas (2,4) since it doesn't affect the ratio.

The simulation shows that the exponents $\boldsymbol{n}$=2 and $\boldsymbol{n}$=4 which have been found to be relevant for the ML growth on flat substrates (Fig. 7) do not provide an adequate simulation of the PSD spectra decay for the saw-tooth substrates after ML deposition. Both the exponents suppress the high-frequency harmonics much stronger than it is observed in the experiment. However one can estimate an effective value of the exponent, $\boldsymbol{n}$, as was suggested in [9]. We found that the exponent $\boldsymbol{n}$=1.6 provided the best match of the fitted and the experimental data (Fig. 10) for both the 200 eV and 700 eV multilayers. The parameter ν which characterizes the strength of the smoothing process increases by a factor

of 1.4 for an ion energy of 700 eV as compared to 200 eV. The value of the exponent is much smaller than ones found for flat multilayers. This indicates a more complicated character of the relaxation processes for the multilayers on saw-tooth substrates as compared to flat ones.

Earlier similar discrepancy between LCM predictions and experiment was reported for smoothing of rippled substrates with ZrO_2 coatings [14]. We recently observed the similar growth behavior for an Al/Zr multilayer deposited on saw-tooth substrates [15]. Such a growth behavior can be caused by large local slope variations for the highly corrugated surface of a saw-tooth substrate. From simple geometrical considerations [16] one can assume that surface concentration of adatoms depends on a local surface slope angle, α. Highly tilted areas receive a smaller amount of particles from the incoming atomic flux, and concentration of adatoms reduces as $\sim \cos\alpha$. A gradient of adatom concentration caused by the surface slope variation induces an additional component of the surface diffusion flux. This effect is weak for the relatively smooth surface of flat multilayers but can contribute significantly in smoothing of highly corrugated surfaces such as saw-tooth substrates. The LCM model is not valid anymore, and a non-linear term should be added into the growth equation. For the case of surface diffusion being a dominating relaxation mechanism, the equation (1) can be rewritten as:

$$\frac{\partial \boldsymbol{h}}{\partial \boldsymbol{t}} = -\nu_4 \nabla^4 \boldsymbol{h} - \lambda \nabla^2 (\nabla \boldsymbol{h})^2 + \eta \qquad (6)$$

The equation (6) was suggested by [16-18] in order to take into account non-linear effects of surface dynamics in particular for the case of epitaxial growth [18]. An additional

non-linear term related to intermixing of Mo and Si layers [19] also should be considered for adequate simulations.

As we discussed earlier [15], the non-linear term $-\lambda\nabla^2(\nabla \boldsymbol{h})^2$ affects a surface and its frequency spectrum in a different way as compared to the linear one ($-\nu_4\nabla^4\boldsymbol{h}$), and this can explain the observed decay behavior of the PSD spectra (Fig. 10). The linear term describes surface diffusion from peaks towards valleys and results in reduction of the amplitude of a surface relief and decay of high frequency harmonics of a Fourier spectrum and hence a PSD function of a surface. Unlike above, the non-linear component of atomic flux causes mass transfer from both peaks and valleys towards slopes and result in widening of the peaks and narrowing of valleys. Similar surface transformation was discussed in [16] for a non-linear term of the Kardar-Parisi-Zhang equation [20]. In the frequency domain, the transformation results in an increase of the high frequency harmonics, and explains why the high frequency peaks of the PSD spectra (Fig. 10) survive longer than predicted by the simple LCM. Nevertheless, the LCM allows finding some effective value of a relaxation exponent. Although physical interpretation of a non-integer exponent is not quite clear, the effective value can serve as an empirical quantitative characteristic of the smoothening process. Full analysis of the multilayer growth using the formula (6) seems promising for more complete simulations, but it requires use of numerical methods since the equation doesn't have an analytical solution, and is not within the scope of this paper.

3.4. Diffraction efficiency of the MBGs

Measurements of diffraction efficiency of the MBG coated with ion beam sputtered Mo/Si multilayers were performed in order to investigate the impact of Kr^+ ion energy on grating performance. Diffraction efficiency of both the 200 eV and 700 eV ion energy gratings was measured using a near-normal incidence geometry and a resonance wavelength of about 13.6 nm. Fig. 11 shows diffraction from the grating, recorded at a fixed incidence angle of 11° by making a detector scan over a diffraction angle. The measurements show that performance of MBGs is strongly dependent on the quality of the groove profile and distortion of the groove profile drastically affects the diffraction efficiency. The 700 eV grating with fairly smoothed groove profile (Fig. 9) has a relatively poor blazing performance, and a significant portion of diffracted energy was directed into the 1st, 0th, and other non-blaze orders. As a result of this the efficiency of the blazed 2nd order does not exceed 21.3%. The 200 eV ion energy grating with less smoothed grooves provides much better concentration of diffracted energy into the blazed 2nd order and demonstrates efficiency around 28.8%. To our knowledge this is a highest efficiency that has been achieved so far for gratings with such a high groove density.

Note that the reflectance of the flat Mo/Si-30 witness is slightly lower for the 200 eV ion case as compared to 700 eV (see insertion in Fig. 11). It is caused partially by the higher roughness of the interfaces which correlates to the roughness observed for the top surface of the multilayer (Fig. 6). Despite this, the 200 eV grating demonstrates much higher diffraction efficiency as compared to the 700 eV ion case (Fig. 11). This clearly shows the crucial importance of groove profile for grating efficiency. Preserving the groove profile during the multilayer deposition is the highest priority issue for further progress in grating

performance and requires new approaches to optimization of ML deposition. Traditional deposition of multilayers on flat substrates aims to increase mobility of surface atoms as much as possible in order to smooth out white noise roughness and obtain perfectly smooth interfaces of a multilayer stack. The results of this work show that a different strategy for the deposition optimization is needed for saw-tooth substrates. The smoothing ability of a multilayer should be precisely tuned, and a balance between smoothening and roughening processes should be found in order to avoid excessive groove shape deterioration. One can sacrifice the interface smoothness to some extend and afford some loss of the ML reflectance of the multilayers in order to preserve the saw-tooth groove profile throughout the multilayer stack, resulting in an optimum and high diffraction efficiency of the MBG.

Summary

The capabilities of an ion-beam sputtering technique to control the growth of Mo/Si multilayers on ultra-dense saw-tooth substrates has been investigated, in order to obtain high diffraction efficiency of the MBG. Highly collimated flux of sputtered atoms allowed minimization of shadowing effects and avoidance of significant perturbations of the multilayer stack as compared to magnetron sputtering techniques.

We found that the energy of ions of a sputtering gas has a strong impact on smoothing ability of the multilayers and performance of multilayer coated gratings. Reduction of the ion energy from 700 eV to 200 eV provided much better replication of a saw-tooth groove profile and resulted in an increase of diffraction efficiency of a MBG by a factor of 1.4. As

a result of the deposition optimization, the efficiency of the 2nd blazed order was increased to approximately 28.8% for a groove density of 7350 lines/mm. This is a new record for high density MBGs.

We found that the growth behavior of Mo/Si multilayers on saw-tooth substrates is very different as compared to flat ones. Smoothening of the saw-tooth substrates is described by an effective relaxation exponent n=1.6 which is much smaller than the one found for multilayers deposited on flat substrates under identical conditions. A non-linear term which is relevant for highly corrugated surfaces should be added into the growth equation for adequate modeling of the surface deposition dynamics.

The smoothing ability of ion beam sputtered Mo/Si multilayers was found to be still too high even at a low energy of the sputtering ions, and resulted in significant degradation of the saw-tooth profile of the grating in the course of the deposition. Further improvement of the deposition process resulting in gaining better control of the energy of the atoms arriving at a substrate is required and should result in even higher diffraction efficiency of high density MBGs.

Acknowledgements

The Advanced Light Source is supported by the Director, Office of Science, Office of Basic Energy Sciences, Material Science Division, of the U.S. Department of Energy under Contract No. DE-AC02-05CH11231 at Lawrence Berkeley National Laboratory.

Disclaimer

This document was prepared as an account of work sponsored by the United States Government. While this document is believed to contain correct information, neither the United States Government nor any agency thereof, nor The Regents of the University of California, nor any of their employees, makes any warranty, express or implied, or assumes any legal responsibility for the accuracy, completeness, or usefulness of any information, apparatus, product, or process disclosed, or represents that its use would not infringe privately owned rights. Reference herein to any specific commercial product, process, or service by its trade name, trademark, manufacturer, or otherwise, does not necessarily constitute or imply its endorsement, recommendation, or favoring by the United States Government or any agency thereof, or The Regents of the University of California. The views and opinions of authors expressed herein do not necessarily state or reflect those of the United States Government or any agency thereof or The Regents of the University of California.

References

1. A. Kotani, Sh. Shin, "Resonant inelastic x-ray scattering spectra for electrons in solids," Rev. Mod. Phys. **73**, 203-246 (2001).
2. D.L. Voronov, M. Ahn, E.H. Anderson, R. Cambie, Ch.-H. Chang, E.M. Gullikson, R.K. Heilmann, F. Salmassi, M.L. Schattenburg, T. Warwick, V.V. Yashchuk, L. Zipp, H.A. Padmore, "High-efficiency 5000 lines/mm multilayer-coated blazed grating for extreme ultraviolet wavelengths," Opt. Lett. **35,** 2615-2618 (2010).

3. D.L. Voronov, M. Ahn, E.H. Anderson, R. Cambie, Ch.-H. Chang, L.I. Goray, E.M. Gullikson, R.K. Heilmann, F. Salmassi, M.L. Schattenburg, T. Warwick, V.V. Yashchuk, and H.A. Padmore, "High efficiency multilayer blazed gratings for EUV and soft X-rays: Recent developments," Proc. SPIE **7802,** 780207 (2010).
4. D.L. Voronov, L.I. Goray, T. Warwick, V.V. Yashchuk, H.A. Padmore, "Optimization of multilayer coated blazed gratings for soft x-ray applications" (to be published).
5. P. Gawlitza, S. Braun, S. Lipfert, and A. Leson, "Ion-beam sputter deposition of x-ray multilayer optics on large areas," Proc. SPIE **6317,** 63170G (2006).
6. James F. Ziegler, Jochen P. Biersack, Matthias D. Ziegler, "SRIM-Stopping and Range of Ions in Matter," *http://www.srim.org*.
7. Y. Fujii, K. I. Aoyama, and J. I. Minowa, "Optical demultiplexer using a silicon echelette grating," IEEE J. Quantum Electron. **QE-16**, 165-169 (1980).
8. P. Philippe, S. Valette, O. Mata Mendez, D. Maystre, "Wavelength demultiplexer: using echelette gratings on silicon substrate," Appl. Opt. **24,** 1006-1011 (1985).
9. W. M. Tong and R. S. Williams, "Kinetics of surface growth: phenomenology, scaling, and mechanisms of smoothening and roughening," Annu. Rev. Phys. Chern. **45**, 401-438 (1994).
10. D.G. Stearns, D.P. Gaines, D.W. Sweeney, E.M. Gullikson, "Nonspecular x-ray scattering in a multilayer-coated imaging system," J. Appl. Phys. **84,** 1003-1028 (1998).
11. E. Spiller, S. Baker, E. Parra, C. Tarrio, "Smoothing of Mirror Substrates by Thin-Film Deposition," Proc. SPIE **3767,** 143-153 (1999).
12. C. Herring, "Effect of change of scale on sintering phenomena," J. Appl. Phys. **21**, 301-303 (1950).

13. M. Moseler, P. Gumbsch, C. Casiraghi, A. C. Ferrari, and J. Robertson, “The ultrasmoothness of diamond-like carbon surfaces,” Science **309**, 1545-1548 (2005).
14. H. Roder, H.-U. Krebs, “Frequency dependent smoothing of rough surfaces by laser deposition of ZrO_2,” Appl. Phys. A **90**, 609–613 (2008).
15. D.L. Voronov, E.H. Anderson, R. Cambie, E.M. Gullikson, F. Salmassi, T. Warwick, V.V. Yashchuk, and H.A. Padmore, “Roughening and smoothing behavior of Al/Zr multilayers grown on flat and saw-tooth substrates,” Proc. SPIE **8139,** 81390B (2011).
16. J. Villain, “Continuum models of crystal growth from atomic beams with and without desorption,” J. Phys. I **1**, 19-42 (1991).
17. T. Sun, G. Guo, M. Grant, Dynamics of driven interfaces with a conservation law, Phys. Rev. A **40**, 6763 6766 (1989).
18. Z.-W. Lai and S. Das Sarma, “Kinetic Growth with Surface Relaxation: Continuum versus Atomistic Models,” Phys. Rev. Lett. **66**, 2348-2351 (1991).
19. D.G. Stearns, P.B. Mirkarimi, E. Spiller, “Localized defects in multilayer coatings,” Thin Solid Films **446**, 37–49 (2004).
20. M. Kardar, G. Parisi, Y.-C. Zhang, “Dynamic Scaling of Growing Interfaces,” Phys. Rev. Lett. **56**, 889-892 (1986).

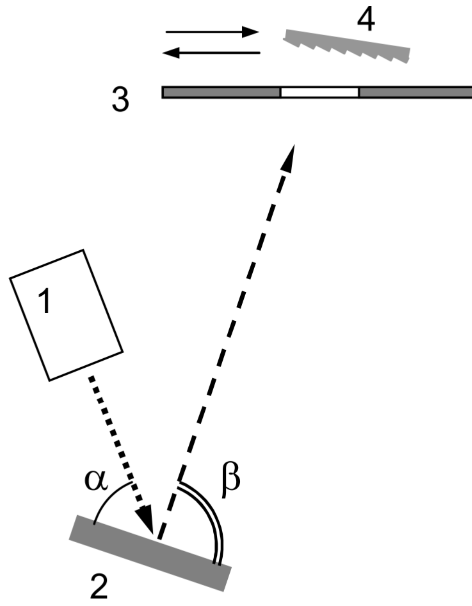

Fig. 1. Schematic of the ion-beam deposition setup: 1- ion gun, 2- target, 3-aperture, 4 – substrate, α is an angle of incidence of the ion beam to a target, β is the takeoff angle.

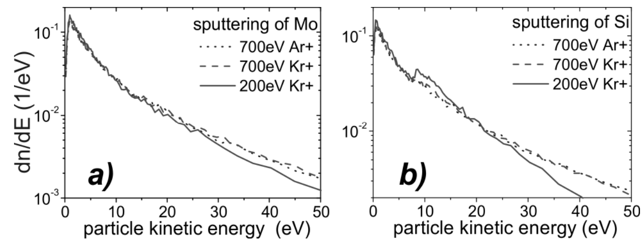

Fig. 2. (color online) SRIM simulated energy distributions for Mo (a) and Si (b) atoms sputtered in the direction of a substrate with Ar^+ and Kr^+ ions with energy of 200 eV and 700 eV. Only the particles sputtered within takeoff angle range of 90º ±20º were counted. All the distributions are normalized to the deposition rate by dividing the raw simulation data by the total number of the particles.

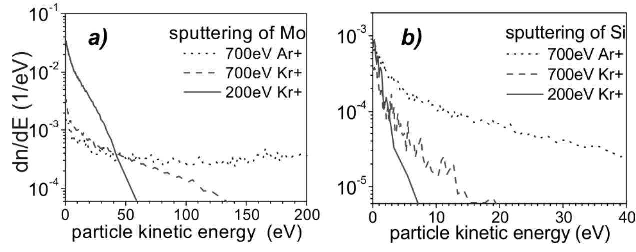

Fig. 3. (color online) SRIM simulated energy distributions of ions and neutrals of the sputtering gas backscattered from Mo (a) and Si (b) targets for an energy of the incident Ar^+ and Kr^+ ions of 200 eV and 700 eV. Only the particles backscattered within a takeoff angle range of 90º ±20º were counted. All the distributions are normalized to the number of sputtered particles.

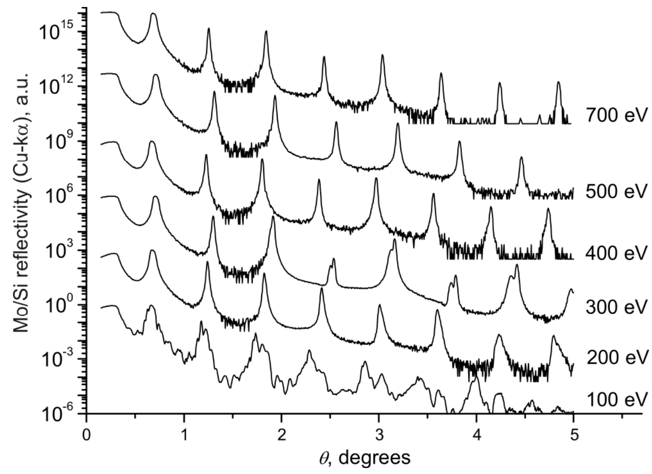

Fig. 4. Small angle x-ray diffraction for ion-beam sputtered Mo/Si-50 multilayers deposited at the Kr^+ ion energy of 100-700 eV. The curves for 200-700 eV are shifted vertically to avoid overlap.

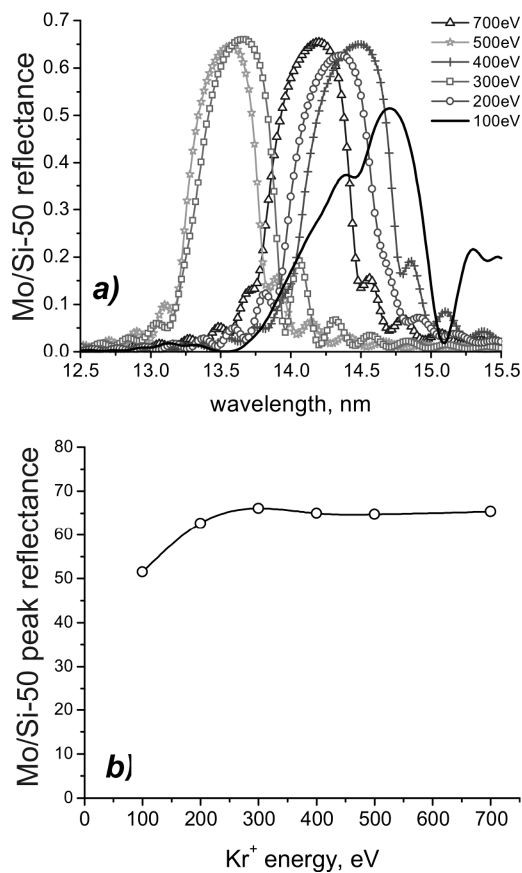

Fig. 5. (color online) Reflectance of ion-beam sputtered Mo/Si-50 multilayers deposited at the Kr^{+} ion energy of 100-700 eV: (a) - dependence of the reflectance on wavelength, and (b) - dependence of a peak reflectance on energy of the sputtering ions.

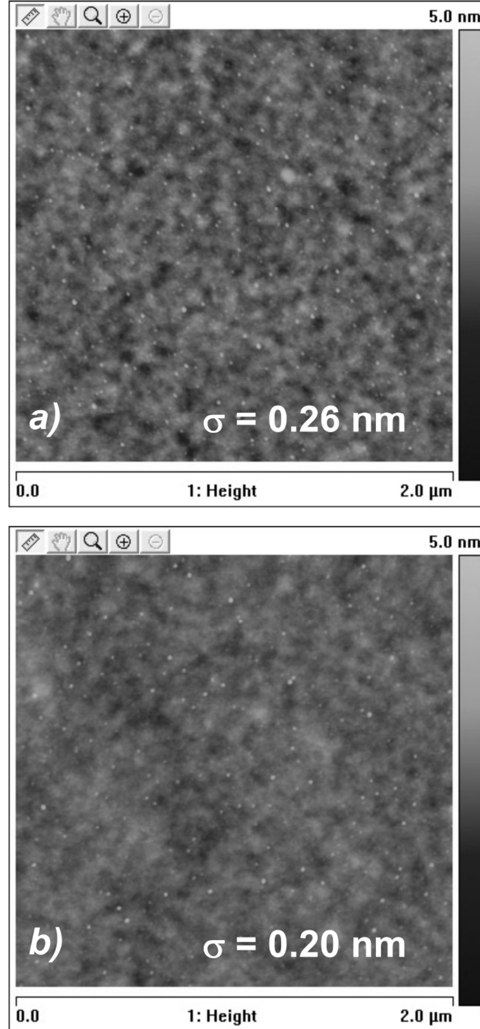

Fig. 6. (color online) AFM images of the top surface of a Mo/Si-30 witness multilayers deposited on flat silicon wafers at a Kr^+ ion energy of 200 eV (a) and 700 eV (b).

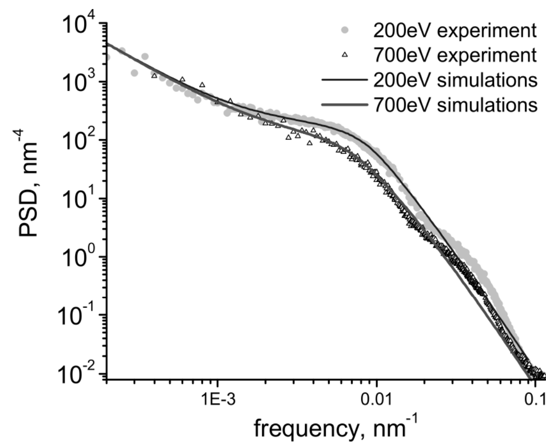

Fig. 7. (color online) PSD spectra of a top surface of the Mo/Si-30 witness multilayers deposited on flat silicon wafers at a Kr^+ ion energy of 200 eV (circles) and 700 eV (triangles). The PSD functions calculated with the formulas (2, 4) 200 eV and 700 eV are shown with thin and thick curves respectively. The PSD of the substrates was modeled as $PSD_{sub}=0.006/\boldsymbol{f}^{1.6}$

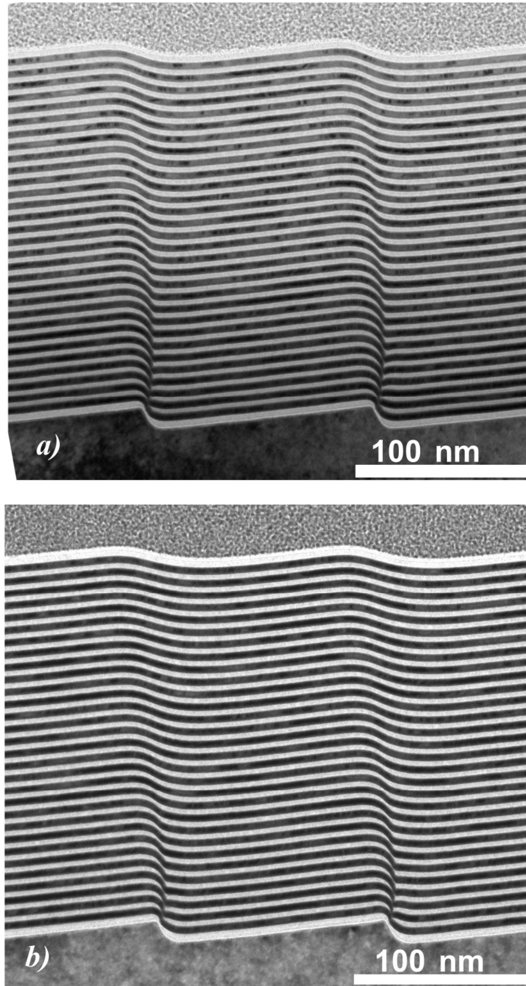

Fig. 8. Cross-sectional TEM images of the MBGs coated with Mo/Si-30 multilayers deposited at Kr^+ ion energies of 200 eV (a) and 700 eV (b)

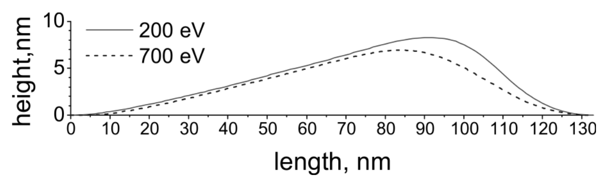

Fig. 9. (color online) Average AFM profiles of the top surface of the MBGs coated with Mo/Si-30 multilayers deposited at a Kr^+ ion energy of 200 eV (solid curve) and 700 eV (dashed curve).

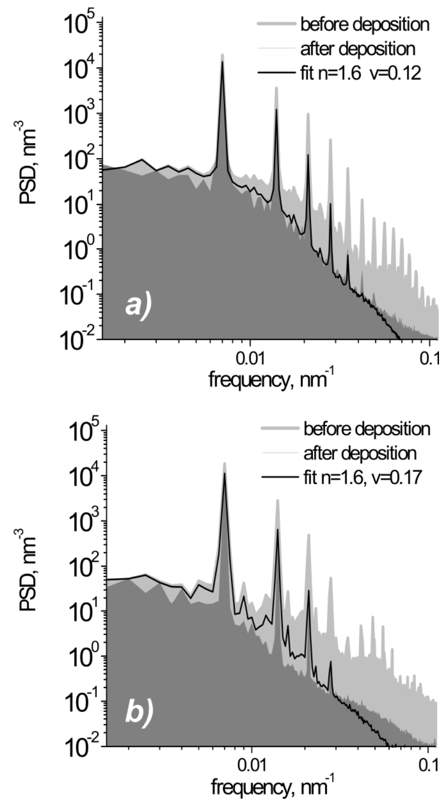

Fig. 10. PSD spectra of saw-tooth substrates before deposition (light grey) and after the deposition (dark grey) of Mo/Si-30 multilayers for a Kr^+ ion energy of 200 eV (a) and 700 eV (b). A black curves show PSD functions calculated for the ML coated gratings with the formulas (4,5).

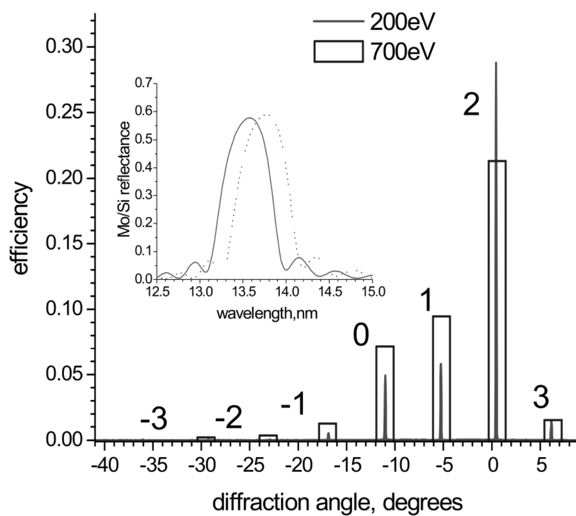

Fig. 11. (color online) Diffraction from the multilayer-coated blazed gratings coated Mo/Si-30 multilayers for Kr^+ ion energy of 200 eV (line) and 700 eV (bars) at the resonant wavelengths of 13.5 nm and 13.65 nm respectively. The insertion shows reflectance of the flat witness MLs deposited at the Kr^+ ion energy of 200 eV (solid curve) and 700 eV (dot curve).

Table 1. Average energy of Mo and Si atoms sputtered in the direction of a substrate with Ar^+ and Kr^+ ions with energy of 200 eV and 700 eV.

Sputtering ions	Sputtered material	
	Mo	Si
Ar^+, 700 eV	17.4 eV	17.2 eV
Kr^+, 700 eV	17.0 eV	15.8 eV
Kr^+, 200 eV	12.6 eV	9.7 eV

Table 2. Average energy of ions and neutrals of the sputtering gas backscattered from Mo and Si targets for the energy of incident Ar^+ and Kr^+ ions of 200 eV and 700 eV.

Sputtering ions	Sputtered material	
	Mo	Si
Ar^+, 700 eV	124 eV	21 eV
Kr^+, 700 eV	39.8 eV	5.2 eV
Kr^+, 200 eV	9.7 eV	1.5 eV

Table 3. Parameters of the model PSD functions (shown in Fig. 7) of the top surface of the flat Mo/Si multilayers, calculated for ion energy of 200 eV and 700 eV with LCM model. A stochastic white noise was considered as the only roughening mechanism.

Growth parameter	Ion energy (eV)	
	200	700
Ω (nm^3)	0.9	0.6
ν_2 (nm)	0.9	1.8
ν_4 (nm^3)	250	310

Table 4. Parameters of the model PSD functions (shown in Fig. 7) of the top surface of the flat Mo/Si multilayers, calculated for ion energy of 200 eV and 700 eV. Additional non-stochastic roughening contribution was taken into account by the LCM model.

Growth parameter	Ion energy (eV)	
	200	700
Ω (nm^3)	0.7	0.5
ν_1 (nm)	-0.1	-0.08
ν_2 (nm)	2.6	3.4
ν_4 (nm^3)	130	200